Compression/dilation of condensed matter vis-à-vis an ideal symmetric material

Isaac C. Sanchez*
McKetta Department of Chemical Engineering, University of Texas, Austin, Texas 78712, USA

(Received 18 September 2018; revised manuscript received 23 October 2018; published 5 December 2018)

Both the isothermal Helmholtz energy and the adiabatic internal energy of condensed matter exhibit minima at zero pressure. As a consequence, the leading term in a density expansion of these two thermodynamic potentials is quadratic in density displacement. When the quadratic term dominates, the material behaves symmetrically in response to isotropic compressive and tensile forces. From an atomistic viewpoint, compressing or stretching atomic bonds to the same degree in a symmetric material increases a corresponding thermodynamic potential by the same amount. The quadratic term contributes to the pressure as a simple cubic equation of state (EOS). Among 29 metals and 17 inorganic solids surveyed, only metallic gold satisfies this simple EOS to the highest measured compressions (>40%). Other solids such as Pt and NaCl also follow this simple EOS to significant compressions and all materials should follow it at low compressions/dilations. A thermodynamic protocol is proposed to extract the bulk modulus B_0 as well as higher order modulus pressure coefficients, B_1, B_2, and B_3, from least squares smoothed data without taking derivatives or by appealing to an EOS model. Reliable and unbiased experimental values of these higher order modulus coefficients have been obtained for 46 solids. These moduli are strongly correlated and satisfy the relationship $B_0^2 B_3 \simeq -2B_0 B_1 B_2$. This relation obtains exactly from an adiabatic EOS based on the Mie (m-n) potential and to a high degree of approximation for the well-known Birch-Murnaghan and Vinet EOS. Truncating the thermodynamic expansion at the fifth order term with only the pressure coefficient B_1 as a parameter, this approximate thermodynamic EOS models experimental values of B_2 and B_3 better than either the third order Birch-Murnaghan or Vinet EOS.

DOI: 10.1103/PhysRevB.98.214103

I. INTRODUCTION

A material densifies in response to isotropic compressive forces according to its compressibility or inversely to its bulk modulus (B). Compression also increases the modulus, the isothermal modulus for isothermal compression or the adiabatic modulus for adiabatic compression. Each type of compression has an associated thermodynamic potential: the Helmholtz potential for isothermal compression and the internal energy for adiabatic compression. The leading term in the expansion of the associated thermodynamic potential is quadratic in density displacement, i.e., the potential varies as $(\rho - \rho_0)^2$ where ρ_0 is the zero-pressure density. Values of $\rho > \rho_0$ correspond to compression and $\rho < \rho_0$ correspond to dilation (negative pressure). For condensed matter, the thermodynamic potential has a minimum at $P = 0$ and small isotropic compressions and dilations to the same degree increase the potential by the same amount. This quadratic term contributes to the pressure (P) as a simple cubic equation of state (EOS): $P = B_0(\rho_r^3 - \rho_r^2)$ where $\rho_r = \rho/\rho_0$ is the density ratio and B_0 is either the zero-pressure isothermal or adiabatic modulus. An ideal symmetric material (ISM) is defined as one that satisfies the above cubic EOS at all compressions.

An ISM is also characterized as one in which the dimensionless pressure coefficient of the bulk modulus at zero pressure, $B_1 \equiv \partial B/\partial P|_{P=0}$, equals 5. Soft materials, such as organic polymers, are characterized by B_1 values of 11 ± 1.5 [1]. As demonstrated herein, for many hard materials, such as metals and inorganics, $B_1 = 4.5 \pm 1$. For mercury, $B_1 \approx 9$ [2]. Rare gas solids display B_1 values of 8 ± 1 [3] and water has a value of about 6 [4]. In 1940, Slater [5] may have been the first to notice that some metals possess B_1 values around 5.

The first correction to the symmetric potential involves the third density derivative on the potential; this dimensionless derivative (f_3) can either be positive or negative. It will be shown that $B_1 = 5 + f_3$, which illustrates the pivotal nature of $B_1 = 5$. A positive value for f_3 indicates that isotropic compression and dilation to the same degree is thermodynamically more punitive for compression, whereas a negative f_3 indicates dilation is more punitive. The crossover between these two qualitatively different behaviors occurs at $B_1 = 5$. Metallic gold is an example of a material that appears to behave symmetrically to very high compressions (>40%).

Another important property of an EOS is the high-pressure limit of the modulus pressure coefficient, $B_1^\infty \equiv \partial B/\partial P)_{P\to\infty}$. Seismological observations on the Earth's core has led to conclusion that $B_1^\infty = 3.0 \pm 0.1$ [6], and $B_1^\infty = 3$ for the ISM. Moreover, the ratio $B_1^\infty/B_1 = 3/5$ has been suggested as characteristic of the lower mantle and core of the Earth [7,8], which is identical to the ISM ratio. Stacey [7] has tabulated the B_1^∞ values for 30+ EOS and only one other EOS yields $B_1^\infty = 3$.

There are many different EOS in the literature and almost all can satisfactorily fit experimental compression data (pressure-density) by proper adjustment of one or more parameters. Usually B_1 is one of the adjustable parameters and

*sanchez@che.utexas.edu

may be one reason why reported values of this parameter often vary by 20%. It is the prediction of higher order pressure coefficients (B_2 and B_3) that makes a clear distinction between various EOS. These higher order moduli play an important role in other arenas, for example, in determining the pressure dependence of the Grüneisen parameter [9]. A thermodynamic protocol is proposed to extract these higher order coefficients from least squares smoothed data without taking derivatives or by appealing to a specific EOS and provides unbiased estimates of these important parameters.

II. THERMODYNAMIC EQUATION OF STATE

A. Isothermal and adiabatic compression/dilation

For isothermal compression, the EOS is obtained from the Helmholtz potential (A):

$$P = -\frac{\partial A}{\partial V}\Big)_T = \rho^2 \frac{\partial A}{\partial \rho}\Big)_T = \rho_0 \rho_r^2 \frac{\partial A}{\partial \rho_r}\Big)_T \equiv \rho_0 \rho_r^2 A', \quad (1)$$

where P is the pressure, V is the volume, ρ is the density, ρ_0 is the zero pressure density, and $\rho_r = \rho/\rho_0$ is the density ratio. The isothermal bulk modulus is given by

$$B = \rho \frac{\partial P}{\partial \rho}\Big)_T = \rho_0\big(\rho_r^3 A'' + 2\rho_r^2 A'\big). \quad (2)$$

At zero pressure $A'(0) \equiv A_1 = 0$ and

$$B(0) \equiv B_0 = \rho_0 A_2 > 0, \quad (3)$$

where $A_2 \equiv A''(0)$. Since $A_1 = 0$ and $A_2 > 0$, this means that the Helmholtz potential passes through a minimum at $P = 0$. The balance between attractive and repulsive forces in condensed matter gives rise to the minimum. Unlike a gas, whose density approaches zero with decreasing pressure, cohesive forces enable condensed matter to sustain a nonzero density not only at zero pressure, but also to negative pressures. As an example, water is able to sustain negative pressures to at least −140 MPa at 42 °C [10]. In principle, condensed matter can sustain negative pressures to the spinodal limit where the bulk modulus vanishes.

Defining a dimensionless thermodynamic potential, $f = A/A_2$, and expanding the potential around $\rho_r = 1$, yields

$$f = f_0 + \frac{1}{2!}(\rho_r - 1)^2 + \frac{f_3}{3!}(\rho_r - 1)^3 + \cdots, \quad (4)$$

where the dimensionless thermodynamic coefficients (f_n) are given by

$$f_n \equiv A_n/A_2 = A_n \rho_0 / B_0, \quad (5)$$

and A_n is the n^{th} derivative with respect to ρ_r on A evaluated at zero pressure.

From Eqs. (1) and (4) the isothermal thermodynamic EOS becomes

$$P = B_0\big(\rho_r^3 - \rho_r^2\big)\left[1 + \frac{f_3}{2!}(\rho_r - 1) + \frac{f_4}{3!}(\rho_r - 1)^2 + \cdots\right]. \quad (6)$$

For adiabatic displacements, the assumption is made that displacement is quasi-isentropic and the EOS is given by

$$P = -\frac{\partial U}{\partial V}\Big)_S = \rho^2 \frac{\partial U}{\partial \rho}\Big)_S \equiv \rho^2 U', \quad (7)$$

where U is the internal energy. Notice the functional similarity between Eqs. (1) and (7). Proceeding as before we arrive at Eqs. (4) and (6) with A replaced by U, but now the modulus is the adiabatic bulk modulus. Unless otherwise noted, all subsequent equations in this paper are applicable to either isothermal or adiabatic compressions/dilations.

B. Ideal Symmetric Response

The ISM is defined as one in which the thermodynamic potential is determined completely by the quadratic term ($f_n = 0,\ n \geqslant 3$):

$$f - f_0 = \tfrac{1}{2}(\rho_r - 1)^2, \quad (8)$$

which yields the following simple cubic EOS:

$$P = B_0 \rho_r^2 f' = B_0\big(\rho_r^3 - \rho_r^2\big). \quad (9)$$

The corresponding bulk modulus is

$$B = \rho_r\left(\frac{\partial P}{\partial \rho_r}\right) = B_0\big(3\rho_r^3 - 2\rho_r^2\big). \quad (10)$$

Note that the modulus vanishes at $\rho_r = 2/3$, at a negative pressure of $-4B_0/27$. This corresponds to the spinodal limit and a magnitude upper bound for the predicted "failure" of the material under isotropic tension. Although a compression or dilation of $|\rho_r - 1| = 1/3$ yields a symmetric response in the thermodynamic potential, it does not in pressure. A compressive displacement of $1/3$ requires a positive pressure four times larger in magnitude, $16B_0/27$.

The pressure coefficient of the modulus for the symmetric material is given by

$$\frac{\partial B}{\partial P} = \frac{\partial \ln B}{\partial \ln \rho} = \frac{9\rho_r - 4}{3\rho_r - 2}, \quad (11)$$

which has the following limiting values at zero and infinite pressures:

$$\frac{\partial B}{\partial P} = \begin{cases} B_1 = 5 & P = 0 \quad \text{or} \quad \rho_r = 1 \\ B_1^\infty = 3 & P \to \infty \quad \text{or} \quad \rho_r \to \infty \end{cases}. \quad (12)$$

It is interesting to note that the ISM ratio $B_1^\infty/B_1 = 3/5$ has been estimated for the lower mantle and the core of the Earth [7,8].

Among 46 metals and inorganics that have been surveyed, elemental gold best exemplifies ideal symmetric behavior. Experimental gold compression data from two studies [11,12] are shown in Fig. 1. The curve through the data is the symmetric EOS, Eq. (9), with $B_0 = 167$ GPa. This modulus value compares favorably with previous experimental determinations of gold's isothermal modulus [13,14].

C. Asymmetric Response

Using Eqs. (1), (2), and (5) yields

$$P = B_0 \rho_r^2 f'(\rho_r), \quad (13)$$

$$B = \rho_r \frac{\partial P}{\partial \rho_r} = B_0\big(\rho_r^3 f'' + 2\rho_r^2 f'\big), \quad (14)$$

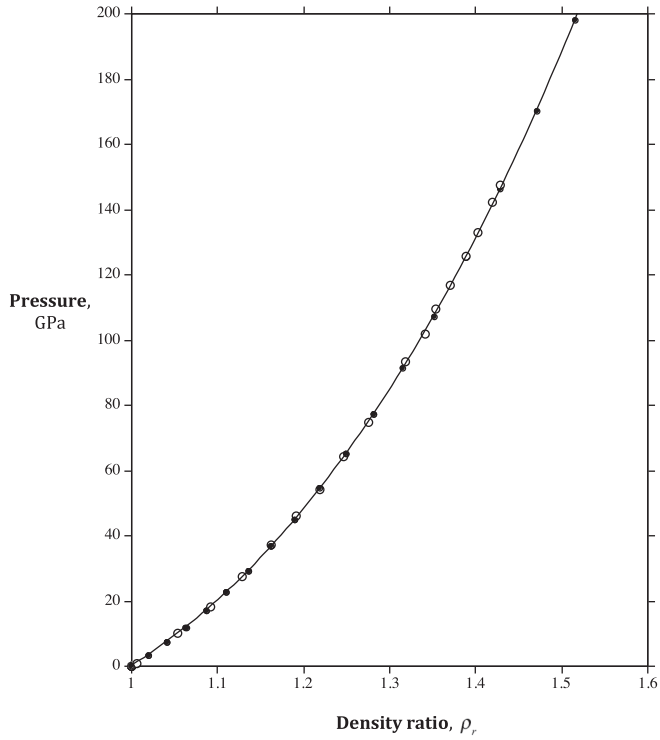

FIG. 1. Experimental gold compression data from two sources; solid circles, Shim *et al.* [11] (smoothed data using BM EOS) and open circles, Akahama *et al.* [12] (unsmoothed data). The line through the data is the ISM EOS, $P = B_0(\rho_r^3 - \rho_r^2)$, with $B_0 = 167.0$ GPa.

which implies

$$f'(1) \equiv f_1 = 0, \quad B(1)/B_0 = f''(1) \equiv f_2 = 1. \tag{15}$$

From Eq. (14), the pressure dependence of the modulus depends on the thermodynamic coefficients as

$$\frac{\partial B}{\partial P} = \frac{\partial \ln B}{\partial \ln \rho} = \frac{\rho_r^2 f''' + 5\rho_r f'' + 4f'}{\rho_r f'' + 2f'}. \tag{16}$$

At zero pressure this becomes ($\rho_r = 1$, $f_1 = 0$, $f_2 = 1$, $f''' \to f_3$):

$$\left.\frac{\partial B}{\partial P}\right|_{P=0} \equiv B_1 = 5 + f_3. \tag{17}$$

For the ISM, $f_3 = 0$ and the pivotal nature of $B_1 = 5$ is immediately recognized. As can be seen from Eq. (4), $f_3 < 0$ indicates that isotropic compression and dilation to the same degree is thermodynamically more favorable for compression, whereas $f_3 > 0$ indicates dilation is more favorable than compression.

Using the recursion relation

$$\tilde{B}_n = \frac{\partial^n B}{\partial P^n} = \frac{\rho}{B}\frac{\partial \tilde{B}_{n-1}}{\partial \rho}; \quad \tilde{B}_n \equiv B_0^{n-1} B_n, \quad n \geqslant 2, \tag{18}$$

along with Eq. (16), the higher order pressure derivatives on the modulus at zero pressure can be obtained:

$$B_0 B_2 = -\left(6 + f_3 + f_3^2\right) + f_4 \tag{19}$$

and

$$B_0^2 B_3 = 60 + 24 f_3 + 9 f_3^2 + 3 f_3^3 - 6 f_4 - 4 f_3 f_4 + f_5. \tag{20}$$

Note for the ISM,

$$f_3 = f_4 = f_5 = 0,$$
$$B_1 = 5, \quad B_0 B_2 = -6, \quad B_0^2 B_3 = 60.$$

III. PROTOCOL FOR DETERMINING MODULUS COEFFICIENTS

It is well known among practitioners that the manner in which experimental compression data are smoothed can have a significant effect on the calculated values of modulus coefficients. For example, if a least squares n^{th} degree polynomial is used, the calculated value of the zero pressure modulus B_0 will generally depend on the value of n as well as other details such as the data range considered and whether or not the fit is forced to pass through the origin. But the statistical problem is even more severe when calculating higher order modulus coefficients. The alternative has been to fit a model EOS to the data, such as the Vinet *et al.* [15,16] EOS, and then use the model to predict the moduli values. This introduces a bias because different models can yield significantly different results. Below a model-independent procedure based on the thermodynamic EOS is described to determine the higher order modulus coefficients.

A. Experimental determination of B_0, B_1, B_2, and B_3

The thermodynamic EOS, Eq. (6), suggests that a plot of P/ρ_r^2 against density displacement, $\rho_r - 1$, should initially be linear with slope B_0 and should clearly reveal the values of the asymmetric coefficients f_3, f_4, ... at sufficiently large compressions. To illustrate, a least-squares fifth order polynomial for lithium compression data [17] is

$$P = 10.4\rho_r^2[(\rho_r - 1) - 0.609(\rho_r - 1)^2 + 0.178(\rho_r - 1)^3]. \tag{21}$$

By inspection, it is seen that $B_0 = 10.4$ GPa. Comparison with Eq. (6) yields

$$f_3 = 2!\ (-0.609) = -1.22,$$
$$f_4 = 3!\ (0.178) = 1.07. \tag{22}$$

From Eqs. (17), (19), and (20), the corresponding modulus coefficients are then obtained

$$B_1 = 3.8\,, \quad B_0 B_2 = -5.2, \quad B_0^2 B_3 = 37. \tag{23}$$

Solids with B_1 values near 5 will exhibit very little curvature in a plot of P/ρ^2 versus $\rho_r - 1$, as illustrated in Fig. 2 for Ag ($B_1 = 5.5$). In contrast, solids such as lithium ($B_1 = 3.8$) with B_1 values further removed from the ISM value of 5, exhibit more curvature.

The proposed protocol is as follows: plot P/ρ_r^2 versus $\rho_r - 1$ and fit the data with a least-squares quadratic or cubic polynomial forced through the origin; a cubic polynomial represents a fifth order fit of pressure to density. If the R-squared coefficient (or other "goodness of fit" metric) does not

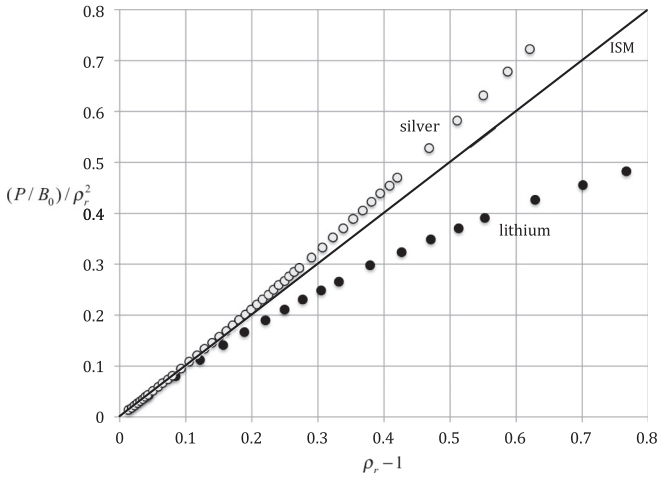

FIG. 2. Data plot illustrates the asymmetric contributions to the thermodynamic EOS. The 45-degree line defines ISM behavior ($B_1 = 5$). A $B_1 < 5$ material such as Li ($B_1 = 3.8$) will exhibit downward curvature, whereas $B_1 > 5$ materials such as Ag ($B_1 = 5.5$) display upward curvature away from the ISM line. Note that the horizontal axis is a compressive strain measure:$(V_0 - V)/V = \rho_r - 1$. Data from Ref. [17].

improve in going from a quadratic to a cubic polynomial, use the quadratic polynomial as the "fit equation." For a quadratic polynomial f_3 is determined and implies $f_4 = 0$. If the best-fit equation is linear, as occurs for gold, then $B_1 = 5$ and $f_3 = f_4 = 0$. Although the proposed statistical methodology works well, it is not necessarily the optimum one.

This protocol was followed for all 46 solids (29 metals and 17 inorganics) with the results summarized in Tables I and II. Also shown in the Tables is the approximation $B_0^2 B_3 \simeq -2B_0 B_1 B_2$. This approximation is consistent with the modulus coefficients for the Mie (m-n) potential and obtains exactly for the ISM. In Appendix A the adiabatic coefficients B_1, B_2, B_3 are calculated for the Mie potential and it is shown that these four coefficients are not independent:

$$B_0^2 B_3 = -2B_0 B_1 B_2. \tag{24}$$

Although rigorously true for the Mie potential and the ISM, this result is assumed to be an approximation. A comparison between calculated and approximated values is illustrated in Fig. 3, and as can be seen, the correlation appears exceptional.

Two of the most widely used models to regress compression data are the Vinet *et al.* [15,16] and the third order Birch-Murnaghan [21] (BM) EOS models. In terms of the reduced pressure (P/B_0), both are one-parameter models (B_1) and their properties are summarized in Appendix B. The BM model also yields the above relationship, Eq. (24), for $B_1 = 16/3, 14/3$, and 4. For other expected values of B_1 the difference is usually much less than 1%. The Vinet EOS also approximates Eq. (24) to within 1 or 2%. However, the predicted individual values of B_2 and B_3 can differ between models and from those determined experimentally. These differences are illustrated in Figs. 4 and 5. In general, the Vinet EOS overestimates while the BM EOS underestimates the magnitude of both $B_0 B_2$ and $B_0^2 B_3$. The better performance of the BM model for $B_1 = 5 \pm 0.5$ values can be attributed to its

TABLE I. Tabulated values of moduli (B_i) and the asymmetric thermodynamic coefficients (f_i) at ambient temperatures. All compression data from Ref. [17] with the exception of Au [11,12] and Pt [18]. See text on how the thermodynamic coefficients are determined from experimental compression data.

Metal	B_0, GPa	B_1	$-B_0 B_2$	$B_0^2 B_3$	$-2B_0 B_1 B_2$	f_3	f_4
Cd	50.6	5.6	6.9	76	76	0.6	0
Ag	106	5.5	6.7	75	75	0.5	0
Zn	60.9	5.5	6.7	74	74	0.5	0
Tl	35.7	5.4	6.6	71	71	0.4	0
Sn	43.7	5.3	6.3	67	67	0.3	0
In	40.2	5.1	6.1	63	63	0.1	0
Pd	196	5.1	6.1	62	62	0.1	0
Pt	277	5.06	6.1	62	61	0.06	0
Pb	44.5	5.06	6.1	61	61	0.06	0
Au	167	5.0	6.0	60	60	0	0
Cr	191	4.8	5.9	56	57	−0.2	0
Cu	139	4.8	5.8	56	56	−0.2	0
Ni	188	4.75	5.8	55	55	−0.25	0
Co	196	4.4	5.8	48	50	−0.6	0
Al	78.8	4.4	5.8	48	51	−0.6	0
Rb	1.99	4.2	5.4	43	45	−0.8	0.5
Th	52.3	4.1	5.2	42	43	−0.9	0.7
Na	5.90	4.1	5.3	42	43	−0.9	0.6
Mg	34.4	4.1	5.2	41	43	−0.9	0.7
Mo	267	4.0	5.0	41	42	−1.0	0.8
K	29.3	4.0	5.4	41	43	−1.0	0.6
Nb	170	3.9	5.1	39	40	−1.1	1.0
Ta	198	3.8	5.0	38	38	−1.2	1.2
V	158	3.8	4.5	37	34	−1.2	1.7
Li	10.4	3.8	5.2	38	37	−1.2	1.1
Be	119	3.7	5.1	36	37	−1.3	1.4
Ti	972	3.7	5.2	37	39	−1.3	1.1
Zr	94.0	3.2	5.4	31	35	−1.8	2.0
Ca	18.4	3.2	5.6	31	36	−1.8	1.8

better representation around the ISM value $B_1 = 5$. Neither model reduces to the ISM EOS at $B_1 = 5$, which implies nonzero, higher-order moduli contributions to the model EOS. This is clearly seen in the series expansions around $\rho_r = 1$ for $B_1 = 5$:

$$P/B_0 = (\rho_r - 1) + 2(\rho_r - 1)^2 + \begin{cases} \frac{17}{27}(\rho_r - 1)^3 - \frac{1}{3}(\rho_r - 1)^4 + \cdots & \text{Vinet} \\ \frac{55}{54}(\rho_r - 1)^3 + \frac{1}{72}(\rho_r - 1)^4 + \cdots & \text{BM} \\ (\rho_r - 1)^3 & \text{ISM} \end{cases} . \tag{25}$$

The BM model nearly generates the correct coefficient of unity for the cubic term and most closely resembles ISM behavior for $B_1 = 5$. All materials should satisfy the ISM EOS at sufficiently low compressions, a condition that the BM EOS almost satisfies for $B_1 = 5$.

B. Truncated thermodynamic (TrTh) EOS

A reasonably accurate thermodynamic EOS obtains by truncating the exact series, Eq. (6) at the f_4 term and replacing

TABLE II. Tabulated values of moduli (B_i) and thermodynamic coefficients (f_i) at ambient temperatures. All compression data from Ref. [17] with the exception of NaCl [19], CsCl [19] and MgO [20]. See text on how the thermodynamic coefficients are determined from experimental compression data.

Inorganic	B_0, GPa	B_1	$-B_0B_2$	$B_0^2B_3$	$-2B_0B_1B_2$	f_3	f_4
KF	12.0	5.5	6.8	75	75	0.5	0
RbCl	5.93	5.3	6.4	69	69	0.3	0
CsCl	17.4	5.2	6.3	66	66	0.2	0
NaCl	23.8	4.85	5.9	57	57	−0.15	0
RbBr	7.68	4.8	5.8	56	56	−0.2	0
LiF	62.9	4.7	5.8	54	55	−0.3	0
RbF	15.1	4.7	5.8	53	54	−0.3	0
CsI	12.4	4.6	5.8	52	53	−0.4	0
LiBr	21.9	4.5	5.7	51	52	−0.5	0
KI	9.40	4.5	5.5	49	50	−0.5	0.2
RbI	9.48	4.5	5.6	49	50	−0.5	0.2
MgO	157	4.35	5.56	47	48	−0.65	0.2
NaBr	20.9	4.3	5.2	44	44	−0.7	0.6
CsBr	21.8	4.1	4.8	42	43	−0.9	0.6
LiCl	32.8	4.0	4.3	38	35	−1.0	1.7
NaI	20.0	3.9	5.2	40	41	−1.1	0.9
LiI	32.8	2.8	5.4	28	31	−2.2	3.1

f_4 by the following approximation:

$$f_4 \simeq f_3(f_3-1)/2 = \tfrac{1}{2}(B_1-5)(B_1-6). \tag{26}$$

This approximation follows by setting $f_5 = 0$ in Eq. (20) and invoking Eq. (24). The TrTh EOS then becomes

$$\frac{P}{B_0} = \left(\rho_r^3-\rho_r^2\right)\left[1+\frac{B_1-5}{2}(\rho_r-1) + \frac{(B_1-5)(B_1-6)}{12}(\rho_r-1)^2\right]. \tag{27}$$

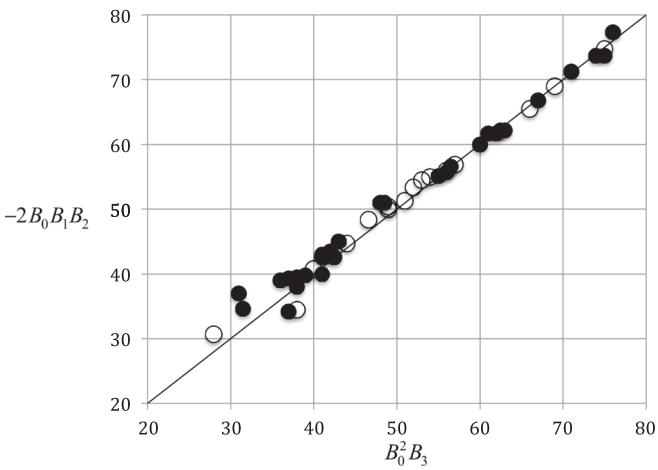

FIG. 3. Test of the correlation $B_0^2B_3 = -2B_0B_1B_2$, which is obeyed by the ISM. Unbiased experimental values from Tables I and II were used to construct this figure. Solid circles are metals and open circles are inorganic solids.

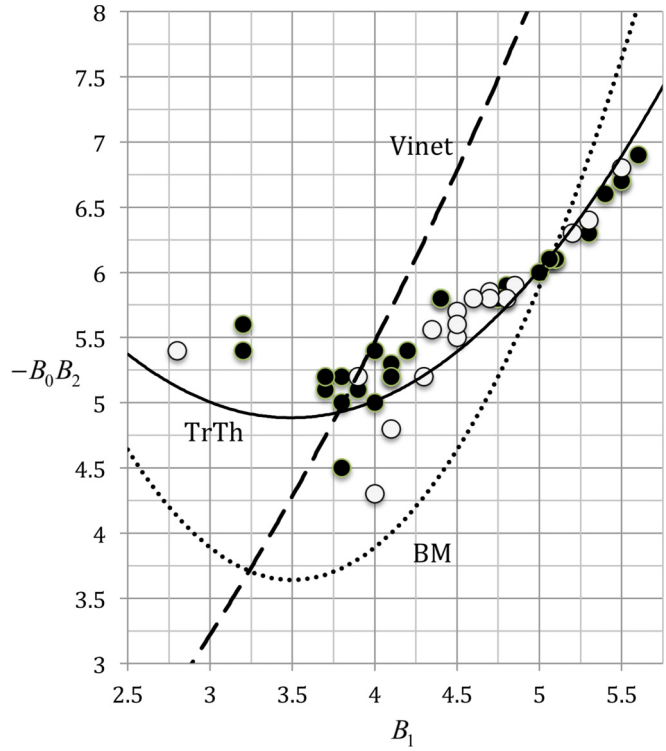

FIG. 4. Predicted values of B_0B_2 compared with unbiased experimental values tabulated in Tables I and II. Solid circles are metals and open circles are inorganic solids. See Appendix B for Vinet and BM formulas used in the calculations. The solid line is Eq. (29). All three equations for B_0B_2 are a function of a single parameter, B_1. Both the third order BM and TrTh equations reach a minimum at $7/2$, whereas the Vinet equation reaches a minimum at -1. The data do hint at a minimum near $7/2$.

The modulus is

$$\frac{B}{B_0} = 3\rho_r^3 - 2\rho_r^2 + \left(\rho_r^3-\rho_r^2\right) \times [f_3(2\rho_r-1) + f_4(\rho_r-1)(5\rho_r-2)/6]. \tag{28}$$

The moduli B_2 and B_3 are obtained immediately from Eqs. (19) and (20):

$$B_0B_2 = -[6+(B_1-5)(B_1-2)/2], \tag{29}$$

$$B_0^2B_3 = B_1[12+(B_1-5)(B_1-2)] = -2B_0B_1B_2. \tag{30}$$

See Figs. 4 and 5 for comparisons with experiment and the Vinet and BM EOS. In general, the Vinet EOS overestimates for $B_1 > 4$ while the BM EOS tends to underestimate the magnitude of B_0B_2 for $B_1 < 5$.

IV. SUMMARY AND CONCLUSIONS

Applying isotropic compression or tension to a material raises an associated thermodynamic potential from its minimum, the Helmholtz potential for isothermal and the internal energy for adiabatic compression/dilations. The identification of a minimum allows for a series expansion of the thermodynamic potential whose leading term is quadratic in density displacement and the expansion can be used

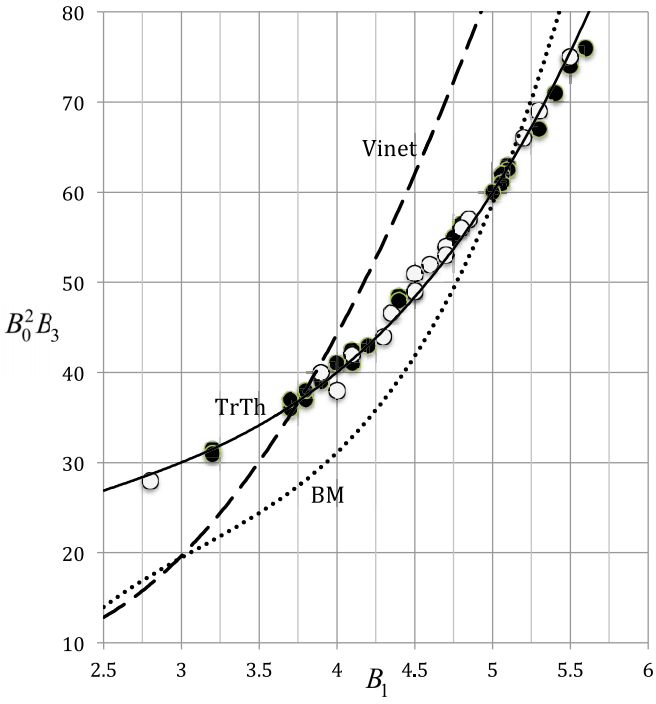

FIG. 5. Predicted values of $B_0^2B_3$ compared with unbiased experimental values tabulated in Tables I and II. Solid circles are metals and open circles are inorganic solids. See Appendix B for Vinet and BM formulas used in the calculations. The solid line is Eq. (30).

for model-independent data analysis. An important result is the ability to extract higher order modulus pressure coefficients (B_1, B_2, and B_3) without taking mathematical derivatives on least squares smoothed data or using an EOS model. These unbiased higher order moduli are tabulated in Tables I for 29 metals and in Table II for 17 inorganic solids.

The strong experimental correlation $B_0^2B_3 \simeq -2B_0B_1B_2$ illustrated in Fig. 3, finds theoretical support when the Mie (m-n) potential is used to describe the energy. As shown in Appendix A, the Mie potential yields this relationship exactly and infers these four moduli are not independent. This relationship also obtains exactly for the ISM and to a high degree of accuracy for the BM EOS (much less than 1% deviation) and the Vinet EOS (average deviation of order 1%).

When $B_1 = 5$, the cubic term in the thermodynamic potential vanishes. It implies the quadratic term should dominate the compressive response to larger compressions than for a material for which $B_1 \neq 5$; i.e., the ISM EOS, Eq. (9), should describe the compressive response to larger compressions. It is indeed surprising the ISM EOS accurately describes gold to very high compressions (>40%) as illustrated in Fig. 1. This suggests, that in addition to $f_3 = 0$, some of the higher order thermodynamic coefficients (f_4, f_5, ...) are zero or very small for gold. From an atomistic viewpoint, $B_1 = 5$ indicates compressing or stretching atomic bonds to the same degree results in comparable thermodynamic potential increases to even larger compressions/dilations than for $B_1 \neq 5$ materials.

Since gold has been widely used as a calibration standard for high-pressure experiments [22,23], it is an important milestone to establish that gold satisfies a very simple cubic EOS state to at least 150 GPa and most likely beyond (see Fig. 1). Gold's modulus properties mimic those of the ISM

$$B_1 = 5, \quad B_0B_2 = -6, \quad B_0^2B_3 = -2B_0B_1B_2 = 60,$$

which serve as guideposts for the compression/dilation response of other materials. Inspection of Tables I and II indicates positive/negative asymmetric contributions to the above ISM values are usually less than 50%.

To third order terms, and with B_1 set equal to 5, the BM equation mimics the ISM EOS [cf. Eq. (25)] quite well. In Appendix B the relationship of the BM EOS with the current TrTh EOS is explored. An important difference between the two is that the BM expansion requires a strain measure, whereas the TrTh EOS does not.

Truncating the thermodynamic expansion, a single parameter EOS is derived, a fifth order polynomial in density, Eq. (27). It compares favorably with the BM EOS, but with the advantage going to the TrTh EOS. Comparisons of the Vinet, BM, and the TrTh EOS with *unbiased* experimental values of B_2 and B_3 are illustrated in Figs. 4 and 5. In terms of predictive performance, TrTh > BM > Vinet.

ACKNOWLEDGMENT

Financial support from the William J. Murray, Jr. Endowed Chair in Engineering is gratefully acknowledged.

APPENDIX A: Mie (m-n) POTENTIAL

The configurational energy contribution to the internal energy at zero pressure is obtained by the usual replacement of the interatomic distance by $\rho^{-1/3}$:

$$f = f_0 + 9\left[\frac{\rho^{n/3}/n - \rho^{m/3}/m}{n-m}\right].$$

The potential is easily generalized as follows: Let the attractive contribution to the configurational energy vary as $-\rho^{\alpha}$ and the repulsive contribution vary as ρ^{β} where the exponents α and β are not restricted to integer values. The only restriction is that $\beta > \alpha > 0$ otherwise a condensed matter state would not exist. Then,

$$f = f_0 + \frac{\rho^{\beta}/\beta - \rho^{\alpha}/\alpha}{\beta - \alpha},$$

which yields

$$f_3 = \alpha + \beta - 3,$$
$$f_4 = (\beta - 3)(\beta - 1) + (\alpha + \beta - 4)(\alpha - 2),$$
$$f_5 = (\alpha + \beta - 5)[(\beta - 3)(\beta - 2) + (\alpha - 4)(\alpha - 1)].$$

Substitution of these f_i into Eqs. (17), (19), and (20) yields

$$B_1 = \alpha + \beta + 2,$$
$$B_0B_2 = -(\alpha + 1)(\beta + 1),$$
$$B_0^2B_3 = 2(\alpha + \beta + 2)(\alpha + 1)(\beta + 1) = -2B_0B_1B_2.$$

The ISM requires $\alpha+\beta=3$ and the only integer values that satisfy this condition are (1,2). Note for $(\alpha,\beta)=(1,2)$, $f_3=f_4=f_5=0$, but in general, for noninteger values of (α,β), $\alpha+\beta=3$ does not guarantee $f_4=f_5=0$.

APPENDIX B: EOS MODULUS PROPERTIES

Vinet *et al.* [15,16]

$$P/B_0 = 3\rho_r^{1/3}\left(\rho_r^{1/3}-1\right)\exp\left[\tfrac{3}{2}(B_1-1)\left(1-\rho_r^{-1/3}\right)\right],$$

$$B/B_0 = 4\rho_r^{2/3}+(3B_1-5)\rho_r^{1/3}-3(B_1-1),$$

$$B_0B_2 = -[(B_1+1)^2/4-7/9],$$

$$B_0^2B_3 = -2B_0B_1B_2+\tfrac{2}{9}(B_1-1),$$

third order Birch-Murnaghan (BM) [21]

$$P/B_0 = \tfrac{3}{2}\rho_r^{5/3}\left(\rho_r^{2/3}-1\right)\left[1+\tfrac{3}{4}(B_1-4)\left(\rho_r^{2/3}-1\right)\right],$$

$$B/B_0 = \tfrac{1}{8}\rho_r^{5/3}\left[3B_1\left(9\rho_r^{2/3}-5\right)\left(\rho_r^{2/3}-1\right)-4\left(27\rho_r^{4/3}-49\rho_r^{2/3}+20\right)\right],$$

$$B_0B_2 = -(B_1-3)(B_1-4)-35/9,$$

$$B_0^2B_3 = -2B_0B_1B_2+\tfrac{1}{9}(3B_1-16)(3B_1-14)(B_1-4).$$

As mentioned in the text, the BM and TrTh EOS exhibit some similarities because both involve thermodynamic expansions; for the BM the elastic energy $E(\varepsilon)$ is expanded as a function of compressive strain ε.

$$E(\varepsilon)=E(0)+\frac{E_2}{2!}\varepsilon^2+\frac{E_3}{3!}\varepsilon^3+\ldots \quad E_n=\left.\frac{\partial^n E}{\partial\varepsilon^n}\right|_{\varepsilon=0}.$$

Strain can be defined in different ways [24] and the BM approach specifically uses Eulerian strain:

$$\varepsilon=\tfrac{1}{2}\left(\rho_r^{2/3}-1\right).$$

The adiabatic contribution of the elastic strain to the pressure is given by

$$P=-\rho^2\left(\frac{\partial E}{\partial\rho}\right)_S=\frac{\rho_r^2}{V_0}\left(\frac{\partial E}{\partial\varepsilon}\right)\left(\frac{\partial\varepsilon}{\partial\rho_r}\right)$$
$$=\frac{\rho_r^{5/3}}{3V_0}\left[E_2\varepsilon+\frac{1}{2}E_3\varepsilon^2+\ldots\right].$$

The third order BM EOS obtains when the elastic energy series is truncated at the third order term, which then yields

$$\frac{P}{B_0}=3\rho_r^{5/3}\left[\varepsilon+\frac{1}{2}\frac{E_3}{E_2}\varepsilon^2\right],$$

where the zero pressure bulk modulus B_0 is identified as $E_2=9B_0V_0$. Using the definitions of the modulus, $B=\rho(\partial P/\partial\rho)$, and the pressure coefficient, $B'=\partial\ln B/\partial\ln\rho$, it can be shown that $B_1=4$ and $E_3/E_2=3(B_1-4)/2$, which when inserted above yields the BM third order EOS.

The second order BM EOS, which only retains the quadratic strain term in the energy expansion, is given by

$$\frac{P}{B_0}=3\rho_r^{5/3}\varepsilon=\frac{3}{2}\rho_r^{5/3}\left[\rho_r^{2/3}-1\right],$$

and yields

$$B_1=4,\quad B_0B_2=-35/9,\quad B_0^2B_3=280/9=-2B_0B_1B_2,$$

i.e., the moduli satisfy Eq. (24) in the text.

In the thermodynamic expansion given in the text, Eq. (6), strain is never defined, but if compressive strain were to be defined simply as

$$\Delta V/V=(V_0-V)/V=\rho_r-1,$$

the ISM EOS, Eq. (9), obtains immediately from above the energy expansion

$$(E_2=B_0V_0,\ E_n=0\quad\text{for all } n\geqslant 3).$$

[1] I. C. Sanchez, J. Cho, and W.-J. Chen, Macromolecules **26**, 4234 (1993).
[2] L. A. Davis, J. Chem. Phys. **46**, 2650 (1967).
[3] S. Gupta and S. C. Goyal, Solid State Commun. **126**, 297 (2003).
[4] I. C. Sanchez, J. Cho, and W.-J. Chen, J. Phys. Chem. **97**, 6120 (1993).
[5] J. C. Slater, Phys. Rev. **57**, 744 (1940).
[6] F. D. Stacey, Phys. Earth Planet. Inter. **128**, 179 (2001).
[7] F. D. Stacey, Rep. Prog. Phys. **68**, 341 (2005).
[8] F. D. Stacey, Phys. Earth Planet. Inter. **142**, 137 (2004).
[9] J. Shanker, K. Sunil, and B. S. Sharma, Phys. Earth Planet. Inter. **262**, 41 (2017).
[10] Q. Zheng, D. J. Durben, G. H. Wolf, and C. A. Angell, Science **254**, 829 (1991).
[11] S.-H. Shim, T. S. Duffy, and T. Kenichi, Earth Planet. Sci. Lett. **203**, 729 (2002).
[12] Y. Akahama, H. Kawamura, and A. K. Singh, J. Appl. Phys. **95**, 4767 (2004).
[13] D. R. Heinz and R. Jeanloz, J. Appl. Phys. **55**, 885 (1984).
[14] O. L. Anderson, D. G. Isaak, and S. Yamamoto, J. Appl. Phys. **65**, 1534 (1989).
[15] P. Vinet, J. Ferrante, J. R. Smith, and J. H. Rose, J. Phys. C **19**, L467 (1986).
[16] P. Vinet, J. Ferrante, J. R. Smith, and J. H. Rose, Phys. Rev. B **35**, 1945 (1987).

[17] G. C. Kennedy and R. N. Keeler, in *American Institute of Physics Handbook*, 3rd ed. (McGraw Hill, New York, 1972), pp. 4-99-104.
[18] M. Yokoo, N. Kawai, K. G. Nakamura, and K. Kondo, Phys. Rev. B **80**, 104114 (2009).
[19] D. L. Decker, J. Appl. Phys. **42**, 3239 (1971).
[20] K. Jin, X. Li, Q. Wu, H. Geng, L. Cai, X. Zhou, and F. Jing, J. Appl. Phys. **107**, 113518 (2010).
[21] F. Birch, Phys. Rev. **71**, 809 (1947).
[22] Y. Akahama, H. Kawamura, and A. K. Singh, J. Appl. Phys. **92**, 5892 (2002).
[23] Y. Fei, A. Ricolleau, M. Frank, K. Mibe, G. Shen, and V. Prakapenka, PNAS **104**, 9182 (2007).
[24] O. L. Anderson, *Equations of State for Geophysics and Ceramic Science* (Oxford University Press, Oxford, 1995).